Iranian Journal of Catalysis 9(1), 2019, 63-70

IRANIAN JOURNAL OF CATALYSIS

Enhancement of photocatalytic degradation of 4-nitrophenol by integrating Ag nanoparticles with ZnO/HZSM-5 nanocomposite

Baharak Divband[a,b], Azadeh Jodaie[c,d,*], Masumeh Khatmian[b]

[a]*Dental and Periodental Research Center, Tabriz University of Medical Sciences, Tabriz. Iran.*
[b]*Inorganic Chemistry Department, Faculty of Chemistry, University of Tabriz, Iran.*
[c]*Applied Chemistry, Islamic Azad University, Sofian Branch, Sofian, Iran.*
[d]*Industrial Nanotechnology research center, Islamic Azad University, Tabriz Branch, Tabriz, Iran.*

Received 21 January 2018; received in revised form 23 December 2018; accepted 2 January 2019

ABSTRACT

In this paper, Ag/ZnO/HZSM-5ternary nanocomposites with different Ag loadings were prepared by the photo precipitation method. The prepared photocatalysts were characterized by XRD, BET, SEM and TEM. The photocatalytic activity of ZnO/HZSM-5 for 4-nitrophenol (4-NP) degradation was increased by silver doping. Effects of various parameters such as the initial concentration of 4-NP, pH and Ag loading on 4-NP degradation were studied. The best activities were obtained for the 3% Ag-10% ZnO/HZSM-5 nanocatalysts at pH 7.9, 1 g L^{-1} of the catalyst and 5 ppm of 4-NP. Langmuir–Hinshelwood (L–H) model was proposed for the rate equation of the 4-NP degradation.

***Keywords**: Photo precipitation method, Ag/ZnO/HZSM-5, Ternary nanocomposites, Photocatalytic oxidation.*

1. Introduction

Contaminations of ground waters by organic chemical molecules create a serious environmental threat. It is due to their toxicity to animals and humans. All possible clean-up methods like microbial direct photodegradation, degradation or even hydrolysis have slight effects on degradation of these compounds [1,2]. Different adsorbents and methods such as sonolysis, solvent extraction, adsorption, precipitation, filtration and electrochemical treatments have been used for removing nitrophenol and other phenolic compounds [3]. All these methods have significant disadvantages such as incomplete removal, production of toxic sludge or other waste products and high-energy requirements [4]. In the last decade, several groups have worked on photocatalytic oxidation of organic compounds to break them to simpler fragments or have researched a complete oxidation of them using different metal oxide-semiconductor materials for their great potential to contribute to solve environmental problems [5,6].

*Corresponding author.
E-mail address: az.jodaei@gmail.com (A. Jodaie)

Semiconductor based (heterogeneous) photo-catalysis, as the most effective advanced oxidation process (AOP), is known as an environmental friendly, safe, cost effective and green process for effective degradation of various harmful organic chemical compounds. This method is based on production of non-selective hydroxyl and superoxide radical oxidants during irradiating a semiconducting material by UV or visible photons with sufficient energy. These radicals can attack pollutants and break them to smaller fragments and finally convert them to H_2O/CO_2 [7,8]. Among several semiconductors, ZnO and TiO_2, which are close to two of the ideal photocatalysts in several respects such as relatively inexpensive cost, provide photo-generated holes with high oxidizing power due to their wide band gap energy [8-10]. As a well-known photocatalyst, ZnO has received much attention in the degradation and complete oxidation of environmental pollutants [11]. The advantage of ZnO is its absorption over a larger fraction of solar spectrum than TiO_2. ZnO, with a band gap of 3.37 eV and a large excitation binding energy (60 meV) at room temperature is a promising material for optoelectronic devices,

transparent conducting and piezoelectric material [12], field emission and surface acoustic wave devices, etc. [13,14]. ZnO exhibits strong n-type conductivity with the electrons moving in the conduction band as charge carriers due to the asymmetric doping limitations and propensity for defects or impurities [13,15-16]. However, its catalytic behavior can be realized under visible excitation by coupling it with CdS and CdSe [17]. P-type doping of ZnO films has been achieved using P [18], N, Zr [19], As [20], Li [21], Sb [22], Pt [23] and Ag [13,24,25] as dopants. It has been found that the photocatalytic performance of ZnO can be greatly improved by constructing Ag–ZnO composite because the rate of electron-transfer process is increased by metal Ag [13,26].

Despite the positive attributes of photocatalysts, poor adsorption properties of semiconductors limit their application. To overcome this limitation, several attempts have been made to improve the efficiency of photocatalysts using suitable supports. Among various supports, zeolites have been widely used due to their unique uniform pores and straight channels [27].

Zeolites modified with transition metal ions have received increasing attention as promising catalysts for a variety of important reactions. Zeolites can serve as hosts to activate transition metal ions, offering a unique ligand system with multiple types of coordination for cations [28, 29]. The aim of this study is to increase the photodegradation efficiency of ZnO/HZSM-5 by adding Ag to produce novel nanocomposites for degradation of 4-NP for the first time. The effects of pH, initial concentration and Ag dosage on 4-NP degradation were also reported.

2. Experimental

HZSM-5 zeolite was synthesized in our laboratory [30]. Zinc acetate dehydrate, ethanol (96%) and silver nitrate were obtained from Merck.

2.1. Measurements

X-ray diffraction patterns (XRD) were collected using a Siemens D500 diffractmeter with Cu kα radiation (λ=1.5418 Å and θ=4-80˚) at room temperature. Scanning electron microscope (Philips XL30) equipped with energy dispersive X-ray (EDX) facility was used to capture SEM images and to perform elemental analysis. The SEM sample was gold coated prior to examination and SEM was operated at 5 kV while EDX analysis was performed at 15 kV. The products have been characterized by transmission electron microscope (TEM) and energy-dispersive X-ray analysis (EDX). TEM studies, combined with EDX, were carried out on a Zeiss LEO 912 Omega instrument, operating at 120 kV. TEM specimens were made by evaporating one drop of solution of sample in ethanol onto carbon coated copper grids. Grids were blotted dry on filter papers and investigated without further treatments. The Brunauer-Emett-Teller (BET) surface area of the catalysts was measured by N_2 adsorption–desorption isotherm at liquid nitrogen temperature using micrometrics ASAP2020. The zeta potential and particle size of samples were measured using Malvern ZS at room temperature. For determination of point of zero charge (pH_{pzc}) of sample, the pH of a series of 50 mL 0.01 M NaCl solutions was set to a value between 2 and 12 by adding HCl 0.1 M or NaOH 0.1 M solution in closed Erlenmeyer flasks. Before adjusting the pH, all solutions were degassed by purging N_2 gas to remove dissolved CO_2. The pH of these solutions was recorded as the initial pH_s (pH_I). Then, 0.2 g of Ag/ZnO/HZSM-5 was added and the final pH (pH_F) was measured after 48 h. Finally, the plots of pH_F versus pH_I and also pH_I versus pH_I were constructed and the intersection of these curves determines the pH_{pzc}.

2.2. Nanocomposite Preparation

In this study, ZnO/HZSM-5nano composite was synthesized by the following reaction:

Proper amounts of $Zn(CH_3CHOO)_2.2H_2O$ were dissolved in 10ml ethanol (96%) at room temperature in an ultrasonic bath for 1 h. Then 0.5 g of HZSM-5 was added and stirred for 12 h (ion exchange method). Then, the mixture was heated under reflux conditions and stirred for 3 h and during reflux, distilled water was added dropwise in order to form the zinc hydroxide inside the zeolite's pores. The precipitate was separated from the solution by centrifugation at 1500 rpm for 5 min and washed with deionized water repeatedly to remove the residual Zn^{2+} and then dried at 80 ℃ for 12 h and finally calcined at 550 ℃ for 4 h. The mass ratio of ZnO: HZSM-5 was 5:100, 7:100, 10:100 & 15:100, which were designed as Z_nHZ (n= 5, 7, 10 & 15), respectively.

For the preparation of Ag/ZnO/HZSM-5 nanocomposites, the aqueous solution of $AgNO_3$ was dropped into the aqueous suspension of ZnO/HZSM-5 under vigorous stirring for 100 minutes in 50 ℃. The reaction mixture was stirred for 2 h under the UV-C (30 w) lamp to reduce adsorbed Ag^+ to Ag nanoparticles. The precipitate was separated from the solution by centrifugation at 1500 rpm for 5 min and washed with deionized water repeatedly to remove the residual Ag^+ and then dried at 70 ℃ for 10 h. The mass ratios of Ag/ZnO/HZSM-5 were (0.5, 1, 2, 1.5, 3, 4, 5 & 10):100, which were designed as $A_nZ_{10}HZ$ (n= 0.5, 1, 1.5, 2, 3, 4, 5 & 10), respectively.

2.3. Catalytic Activity

Degradation of 4-nitrophenol (4-NP) was chosen as the reaction to quantify the photocatalytic reactivity of each sample. The experiments were carried out with 100 ml 4-NP of solutions. Prior to illumination, the reaction suspension was first magnetically stirred in the dark for 15 min to ensure the establishment of adsorption/desorption equilibrium of the concerned chemical substances on the surface of the catalysts. Then, the Pyrex glass beakers were put under the ultraviolet light with one mercury lamp, Philips 8 W (UV-C) in the appropriate stirring. 1 g L^{-1} of catalysts was added to the 5 ppm solution of 4-NP and the pH of the solution was initially 7.9. The analysis of concentration of 4-NP in the filtered solution was performed by means of a Shimadzu UV-240 spectrophotometer.

The absorption band around 315 nm (for the 4-NP) decreased as a function of time for each catalyst. This can be attributed to the oxidative degradation of the 4-NP by the catalysts. According to the adsorption experiments, the percentage of 4-NP adsorbed on the catalyst surface was determined from the Eq. (1):

$$\text{Degradation (\%)} = [(C_0 - C_t)/ C_0] \times 100 \qquad (1)$$

where C_0 is the initial concentration of 4-NP and C_t is the concentration of 4-NP at time t (min).

3. Results and Discussion

3.1. Catalysts Characterization

3.1.1. XRD patterns

X-Ray diffraction of ZnO/HZSM-5 with different amounts of ZnO loading is depicted in Fig. 1. The characteristic peaks of the ZSM-5 have good agreement with the XRD data of references (JCPDS No. 01-084-0385) [31,32]. The presence of weak new peaks in 2 θ values of 31.2°, 34° and 36.2° in the ZnO/HZSM-5 patterns indicate incorporation of ZnO into the zeolite structure [27]. The diffraction peaks of ZnO with the quartzite structure (JCPDS No. 36-1451) appear when the ZnO loading exceeds 5 wt% and develop obviously when the ZnO loading increases. It is believed that high loading amounts lead to the formation of ZnO nanoparticles on the external surface of HZSM-5. No characteristic peaks of other impurities were detected in the patterns. With increasing the amounts of ZnO loading, the effective interaction between zeolite framework and ZnO structure occurred. In our previous work [30], ZnO nanoparticles was aggregated on the external surface of the zeolite so at 7% loading, the intensive peaks at ZnO appeared in XRD patterns, but using this new method, ZnO clusters were formed into the pores and channels of the zeolite, so up to 10%, the weak peaks of ZnO appeared in XRD patterns.

Fig. 2 represented the X-Ray diffraction of Ag/ZnO/HZSM-5 with different amounts of Ag loading. By increasing the Ag amount, the crystallinity of ZSM-5 was decreased. The reason for this decrease maybe attributed to partial dealumination due to heating during ion exchange process in the presence of water.

3.1.2. BET, SEM, TEM and EDS investigations

HZSM-5 zeolite was used as the host to confine the ZnO clusters and Ag atoms because of its well-ordered pores. The BET specific surface area of HZ, Z_5HZ, Z_7HZ, Z_{10}HZ, A_2Z_{10}HZ, A_3Z_{10}HZ&$A_{10}Z_{10}$HZ are 307, 292, 285, 272, 269, 266 & 209 m^2 g^{-1}, respectively. As seen, the BET values decrease with increasing amounts of ZnO and Ag loadings. This suggests that the pores of zeolite are partly occupied by ZnO clusters and also Ag particles. By introducing nanoparticles into the sub-nano holes of zeolite (Table 1), the volume and area

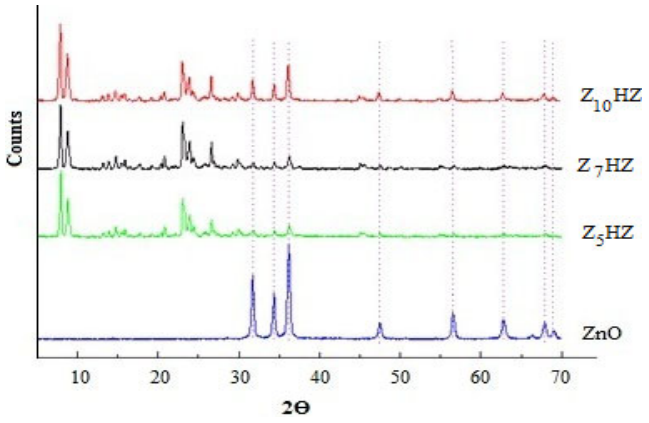

Fig. 1. Powder XRD patterns of ZnO, Z_5HZ, Z_7HZ and Z_{10}HZ.

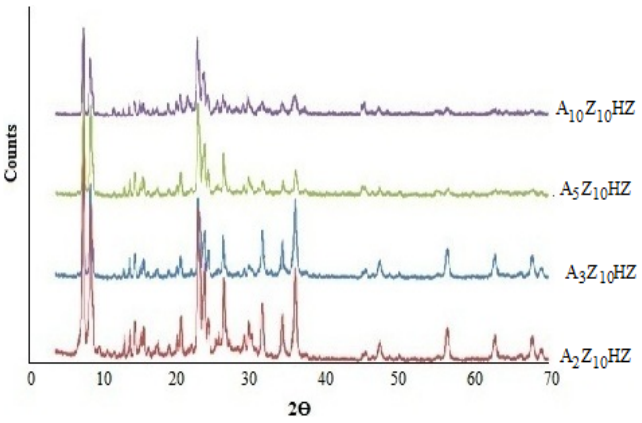

Fig. 2. Powder XRD patterns of A_2Z_{10}HZ, A_3Z_{10}HZ, A_5Z_{10}HZ and $A_{10}Z_{10}$HZ.

Table 1. Structural properties of HZSM-5 based nanocomposites.

Samples	BET Surface Area ($m^2\ g^{-1}$)	Micropore Volume ($cm^3\ g^{-1}$)	Micropore Area ($m^2\ g^{-1}$)	External Surface Area ($m^2\ g^{-1}$)
HZ	307	0.068	131.607	175.979
$Z_{10}HZ$	272	0.087	163.213	105.745
$A_3Z_{10}HZ$	266	0.085	161.719	104.856

of micropores increase. This indicates the large particles enter the holes and zeolite channels, but the decrease in the external surface area is due to occupation with nanoparticles and silver.

The morphologies of the as-prepared products were investigated using TEM. Fig. 3 (A) shows the TEM image of $A_3Z_{10}HZ$ nanoparticles. The black spots on this image denote the Ag particles.

The SEM image of as-synthesized$A_3Z_{10}HZ$ is also shown in Fig. 3 (B). It is clear that the sample is composed of lots of spheres with the diameter in the range of 2-5 µm. The average particle sizes of ZnO nanoparticles are 30-50 nm.

Energy dispersive X-ray spectroscopy (EDS) analysis (Fig. 3 (C)) confirms that $A_3Z_{10}HZ$ nanocomposite materials consist Ag, Zn, Si, Al and oxygen. The presence of Cu and carbon signals arise from the TEM gird. Apart from that, no other elemental peaks could be detected.

3.2. Photocatalytic studies of 4-NP

Total 4-NP removal is composed of two parts, adsorption on photocatalyst and photocatalytic degradation. As shown in Fig. 4, before UV irradiation, with decreasing the amount of the ZnO loading in ZnO/HZSM-5 nanocomposites (from 15 wt.% to 5 wt.%), the concentration of 4-NP reduced, indicating that the degree of adsorption of 4-NP on nanocomposite increased. ZnO does not exhibit considerable adsorption capacity (BET= 5 $m^2\ g^{-1}$, [30]) compared to HZSM5 zeolite (BET= 307 $m^2\ g^{-1}$), so the ZnO particles were introduced into the pores and the extra surface of HZSM-5, reducing the surface area as well as 4-NP adsorption. On the other hand, after UV irradiation when the amount of ZnO loading increased from 5 wt.% to 10 wt. %, there was an increase in the number of particles; hence, the degradation rate gradually increased.

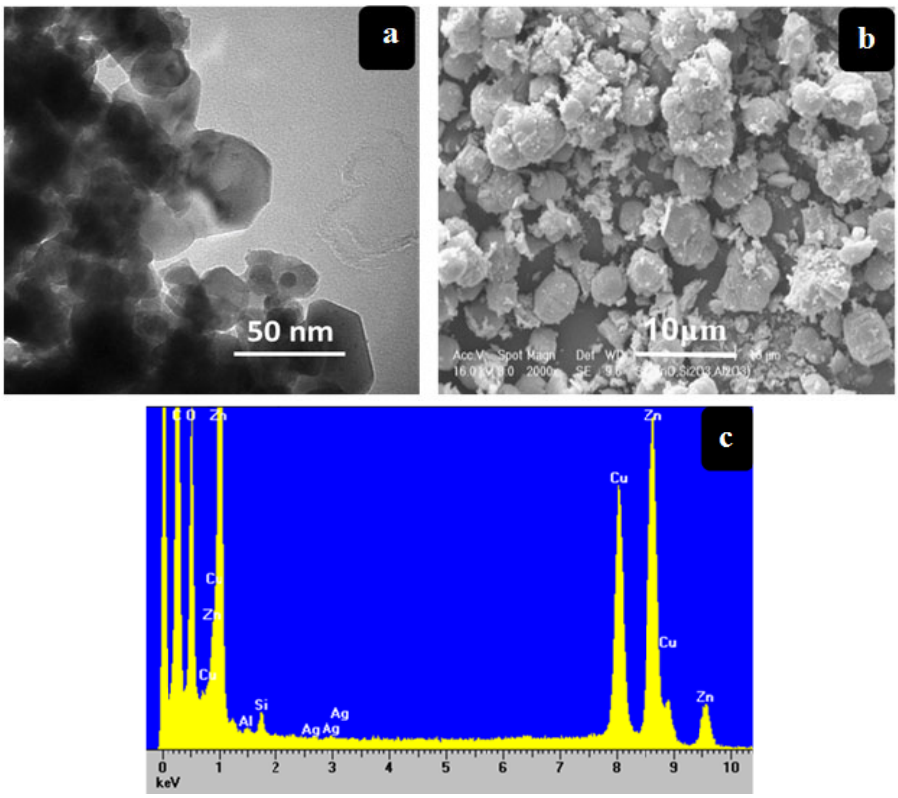

Fig. 3. TEM images of (a) $A_3Z_{10}HZ$ nanoparticles, (b) SEM image of $A_3Z_{10}HZ$ and (c) EDS spectrum of $AZ_{10}HZ$.

Free ZnO or growth of ZnO particle size may also be due to the decrease in degradation rate at higher loadings (>10%). These experiments demonstrated that the nanocomposites with very low amount of ZnO loading did not show sufficient photocatalytic activity and also both HZSM-5 zeolite and photocatalyst such as ZnO were needed for the effective destruction of 4-NP. The 4-NP molecules adsorbed into the pores of HZSM-5 could efficiently spill over to ZnO nanoparticles, producing high photocatalytic reactivity.

3.2.1. Effect of Ag

In this study, incorporation of Ag onto ZnO/HZSM-5 was found to markedly improve the conversion. In other words, the photocatalytic activity of Ag/ZnO/ZSM-5 is higher than that of ZnO/HZSM-5, revealing that silver plays an important role in the conversion of organic compounds. For the purpose of comparison, the photo oxidation of 4-NP was carried out over several Ag loading catalysts. The 4-NP degradation increased with an increase in Ag loading (Fig.5). The order of catalytic activity was as follows: A_3 Z_{10}HZ > A_2 Z_{10}HZ> $A_{1.5}Z_{10}$HZ> A_1Z_{10}HZ> $A_{0.5}Z_{10}$HZ> A_4 Z_{10}HZ> A_5 Z_{10}HZ> A_{10} Z_{10}HZ. Despite having higher silver loading (4-10wt %), Ag/ZnO/ZSM-5 showed a relatively lower activity. This result indicated that the active metal content alone does not result in a good photocatalyst. Participating factors include metal dispersion, available surface area, exchange site and other types of active sites that could catalyze the reaction, such as acid sites [30]. Also, another possible reason is that, at high concentration, silver particles act as recombination centers, this is caused by the electrostatic attraction of positively charged holes and negatively charged silver [33].

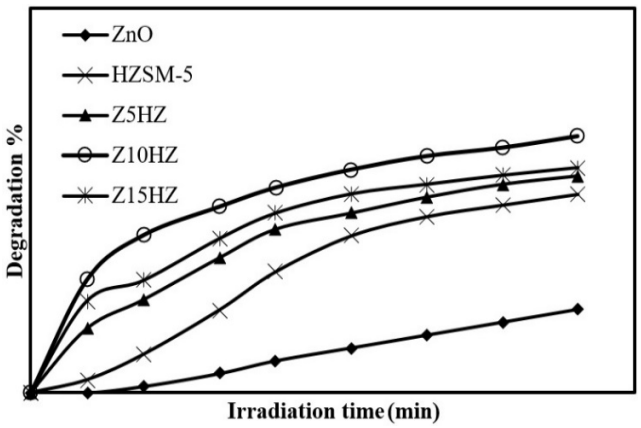

Fig. 4. Effect of ZnO content on the photocatalytic degradation of 4-NP.

3.2.2. Photocatalytic processes

It is well known that the photocatalytic degradation of organic pollutants in the solution is started by photoexcitation of the semiconductor, followed by the formation of an electron – hole pair on the surface of photocatalyst (Eq. (2)). After the decomposition of water, very reactive ȮH groups can also be formed either by (Eq. (4)) or by the reaction of the hole with OH^-(Eq. (6)). The ȮH is as non-selective oxidant that leads to degradation of organic compounds [16,18,34]:

$$ZnO + hv\ (UV) \rightarrow ZnO\ (e_{CB}^- + h_{VB}^+) \quad \textbf{(2)}$$

$$Ag \rightarrow Ag^+ + e^- \quad \textbf{(3)}$$

$$e^- + O_2(ads) \xrightarrow{H^+} {}^\circ O_2^- \rightarrow {}^\circ O_2H \xrightarrow{{}^\circ O_2H} O_2 + H_2O_2$$
$$\xrightarrow{e^-} O_2 + {}^\circ OH + OH^- \quad \textbf{(4)}$$

$$Ag^+ + e^- \rightarrow Ag \quad \textbf{(5)}$$

$$h_{VB}^+ + OH^- \rightarrow {}^\circ OH \quad \textbf{(6)}$$

$${}^\circ OH + 4-NP \rightarrow Oxidation\ of\ 4-NP \quad \textbf{(7)}$$

3.2.3. Effect of concentration of 4-NP

The effect of initial concentration of 4-NP on its photodegradation was studied at different concentrations (Fig. 6). It was observed that the percent degradation gradually decreased with an increase in initial concentration. As the concentration of 4-NP solution increases, the photons get intercepted by dye molecules before they reach the catalyst surface, decreasing the absorption of photons by the catalyst. Hence, the generation of relative amounts of OH^- and $O^{2-\circ}$ on the surface of the catalyst decreases. Thus, the 4-NP degradation efficiency decreases as the 4-NP concentration increases [35].

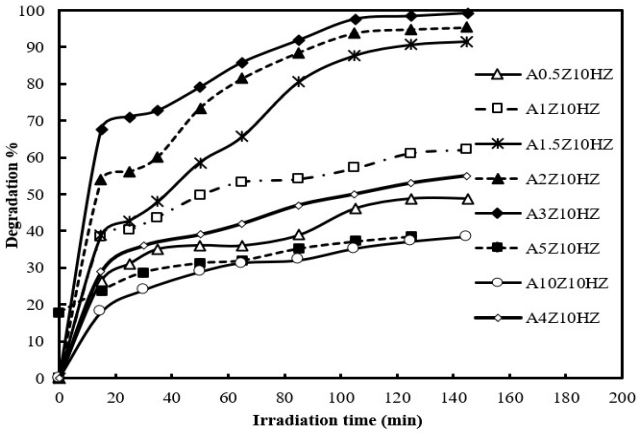

Fig. 5. Effect of Ag% on the photocatalytic degradation of 4-NP.

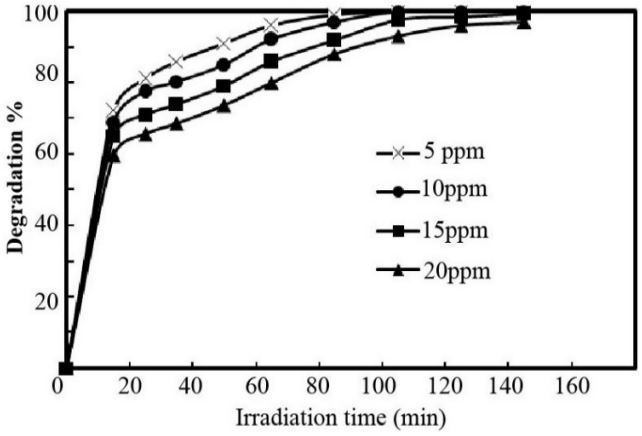

Fig. 6. Effect of initial concentration of 4-NP on photocatalyst activity.

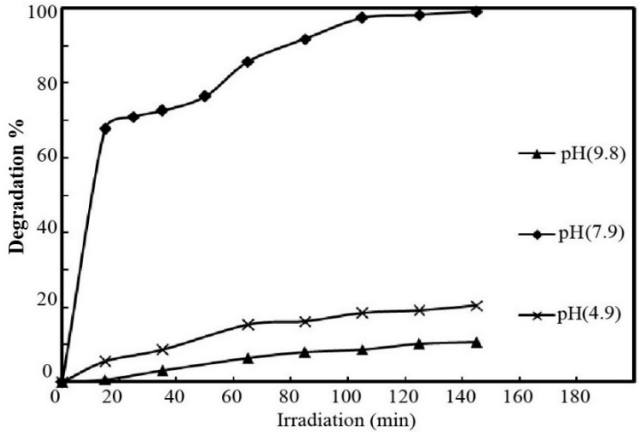

Fig. 7. Effect of pH on the photocatalytic degradation of 4-NP.

3.2.4. Influence of initial solution pH

The pH is an important parameter for photocatalytic processes. The properties of solid–electrolyte interference, i.e. the electrical double layer, can become modified as the pH of the medium changes. Consequently, the effectiveness of the adsorption–desorption process and the separation of the photogenerated electron–hole pair are also substantially affected [36,37]. In the present system with an increase in pH from 4.8 to 7.9, the reaction rate is increased. But, with further increase in pH (9.8), the rate of photo degradation decreases (Fig. 7). The semiconductor ZnO is amphoteric in nature. At the acidic pH, ZnO can react with acids to produce the corresponding salt, while at alkaline pH, it can react with a base to form complexes like $[Zn(OH)_4]^{2-}$[27,30]. The effect of pH on the photocatalytic reaction can be explained on the basis of the zero-point charge (pzc) of Ag/ZnO/HZSM-5 photocatalyst and the adsorption of the pollutants on the photocatalyst in different pH values. The isoelectric point (IEP) is the pH at which the zeta potential is zero.

The IEP of Ag/ZnO/ZSM-5 photocatalyst depends on the acid-alkali properties of surface hydroxyl groups [38]. The pzc of synthesized photocatalyst was at pH~9. It is believed that the surface of photocatalyst is positively charged in pH < 9 by the adsorbed H^+ ions on the semiconductor surface, whereas it is negatively charged under alkaline conditions (pH > 9) by the adsorbed OH^- ions on the semiconductor surface.

The anionic or cationic form of the organic compound affects the photodegradation efficiency. This efficiency is enhanced or inhibited by the electrostatic attraction or repulsion, respectively, between the photocatalyst's surface and the organic molecule [39]. The increase of photodegradation rate at pH 7.9 shows that a part of organic compound degradation was favored by the positively charged photocatalyst.

At pH value of 7.9 the surface of photocatalyst acquires positive charges and thus has the ability to attract the negatively charged organic compounds on its surface, because the pKa of 4-NP is 7.05 [40], so 4-NP exists in a molecular form, thereby increasing the degradation rate at pH 7.9. It can be shown that hydrogen from nondissociated 4-NP is attracted by oxygen from zeolite framework [38]. This hydrogen bonding plays a significant role in adsorption and mobilizing of pollutants on the active sites of ZnO. Also, at lower pH than pHpzc, the attraction forces between H^+ ions absorbed on the catalyst and electrons of nitrogen or oxygen atoms of 4-NP increases and a large amount of 4-Np is adsorbed on the catalyst surface [39-40]. Due to partial protonation of free electrons of 4-NP at stronger acidic conditions, by increasing the repulsive forces of protonated oxygen or nitrogen atoms with positive surface catalyst, less pollutant molecules can reach the catalyst surface where hydroxyl radical will form, hence the degradation efficiency decreases [41-43].

3.3. Kinetic model

The kinetic model for heterogeneous photocatalytic can be used in accordance with the Langmuir-Hinshelwood kinetic expression [44-47]. This model for 4-NP degradation can be written as Eqs. (8) and (9):

$$r = -\frac{d[C]}{dt} = k_c \frac{k_{ads}[C]}{1+k_{ads}[C]_0} = k_{obs}[C] \quad (8)$$

$$\frac{1}{k_{obs}} = \frac{1}{k_{ads}k_c} + \frac{[C]_0}{k_c} \quad (9)$$

where $[C]_0$ is the initial concentration of 4-NP (mg L^{-1}), k_c is the rate constant of surface reaction (mg $L^{-1}min^{-1}$), k_{ads} is the Langmuir–Hinshelwood adsorption equilibrium constant (L mg^{-1}), and k_{obs} is the pseudo-first-order rate constant (min^{-1}). When initial concentrations were plotted versus $1/k_{obs}$, the rate constant of surface reaction and the adsorption

equilibrium constant were determined to be k_c= 0.557 mg L^{-1} $min^{-1}$and k_{ads}= 0.163 L mg^{-1}, respectively. The good regression coefficient (R^2= 0.989) indicated that the photocatalytic degradation of 4-NP by the Ag/ZnO/HZSM-5 fitted into the Langmuir–Hinshelwood kinetic expression well.

4. Conclusions

In this paper, Ag/ZnO/HZSM-5 ternary nanocomposites with different Ag amounts were successfully synthesized by the photo precipitation method for the first time. The catalytic activity of nanocomposites was tested by carrying out the 4-NP degradation. The efficiency of the studied system in terms of the degradation rate followed the order: Ag/ZnO/HZSM-5> ZnO/HZSM-5> HZSM-5> ZnO.

The obtained results indicated that the photodegradation rate of 4-NPh was affected by the initial 4-NP concentration, the pH of solution and the amount of Ag. The proper addition of Ag could improve and accelerate the photocatalytic degradation rate. The present study has shown that Ag/ZnO/HZSM-5 containing 3 %wt of Ag and 10 %wt of ZnO presented a higher activity for the complete photo oxidation of 4-NP. The best degradation was achieved at natural pH (7.9).

The photocatalytic degradation of 4-NPh followed the pseudo first-order kinetics according to the Langmuir–Hinshelwood model. The good regression coefficient (R^2= 0.989) indicated that the photocatalytic degradation of 4-NP by the Ag/ZnO/HZSM-5 fitted into the Langmuir–Hinshelwood kinetic expression well.

Acknowledgements

The authors would like to acknowledge the financial support from Iran National Science Foundation (INSF 92023917).

References

[1] C. Hariharan, Appl. Catal. A 304 (2006) 55–61.
[2] A. Besharati-Seidani, Iran. J. Catal 6 (2016) 447-454.
[3] A.R. Nezamzadeh-Ejhieh, M. Khorsandi, J. Hazard. Mater. 176 (2010) 629–637.
[4] A. Jodaei, D. Salari, A. Nieaei, M. Khatamian, S.A. Hosseini, J. Environ. Sci. Health A 46 (2011) 50–62.
[5] S. Rasalingam, R. Peng, R.T. Koodali, J. Nanomater. 2014 (2014) Article ID 617405, 42 pages.
[6] M. Giahi, A. Hoseinpour Dargahi, Iran. J. Catal. 6 (2016) 381-387.
[7] H. Derikvandi, A. Nezamzadeh-Ejhieh, J. Hazard. Mater. 321 (2017) 629–638
[8] H. Zabihi-Mobarakeh, A. Nezamzadeh-Ejhieh, J. Ind. Eng. Chem. 26 (2015) 315–321.
[9] A. Bagheri Ghomi, Iran. J. Catal. 6 (2016) 293-296.
[10] A. Nezamzadeh-Ejhieh, M. Bahrami, Des. Water Treat. 55 (2015) 1096–1104.
[11] H. Fallah Moafi, Iran. J. Catal. 6 (2016) 281-292.
[12] K. Katoa, T. Komaki, M. Yoshino, H. Yukawa, M. Morinaga, K. Morit, J. Eur. Ceram. Soc. 24 (2004) 139-146.
[13] M. Khatamian, A.A. Khandar, B. Divband, M. Haghighi, S. Ebrahimiasl, J. Mol. Catal. A: Chem. 365 (2012) 120-127.
[14] B. Hahn, G. Heindel, E. Pschoor-Schoberer, W. Gebhardt, Semicond. Sci. Technol. 13 (1998) 788-791.
[15] H.R. Pouretedal, M. Fallahgar, F.S. Pourhasan, M. Nasiri, Iran. J. Catal. 7 (2017) 317-326.
[16] Y. Sun, P. Xu, C. Shi, F. Xu, H. Pan, E. Lu, J. Electron. Spectrosc. Relat. Phenom. 114–116 (2001)1123–1125.
[17] J. Nayak, S.N. Sahu, J. Kasuya, S. Nozaki, Appl. Surf. Sci. 254 (2008) 7215–7218.
[18] Y. Liu, C. Liu, Q. Rong, Z. Zhang. Appl. Surf. Sci. 220 (2003) 7–11.
[19] X. Duan, Y. Zhao, R. Yao, Solid State Commun, 147 (2008) 194-197.
[20] S.B. Zhang, S.H. Wei, A. Zunger, Phys. Rev. B 63 (2001) 075205.
[21] J. Zhao, C. Xie, L. Yang, S. Zhang, G. Zhang, Z. Cai. Appl. Surf. Sci. 330 (2015) 126-133.
[22] Q.J. Feng, S. Liu, Y. Liu, H.F. Zhao, J.Y. Lu, K. Tang, R. Li, K. Xu, H.Y. Guo. Mater. Sci. Semicond. Process. 29 (2015) 188-192.
[23] L. Vafayi, S. Gharibe, Iran. J. Catal. 5 (2015) 365-371.
[24] A. Jodaei, D. Salari, A. Niaei, M. Khatamian, N. Çaylak, Environ. Technol. 32 (2011) 395–406.
[25] B. Khodadadi, Iran. J. Catal. 6 (2016) 305-311.
[26] S. Jafari, A. Nezamzadeh-Ejhieh, J. Colloid Interf. Sci. 490 (2017) 478-487.
[27] H. A. Rangkooy, M. Nakhaei Pour, B.F. Dehaghi, Korean J. Chem. Eng. 34 (2017) 3142–3149
[28] M.M. Ba-Abbad, M.S. Takriff, A. Benamor, A.W. Mohammad, Adv. Powder Technol. 27 (2016) 2439–2447.
[29] M. Khatamian, M. Fazayeli, B. Divband, Mater. Sci. Semicond. Process. 26 (2014) 540–547.
[30] M. Khatamian, B. Divband, A. Jodaei, Mater. Chem. Phys. 134 (2012) 31-37.
[31] Z. Shams-Ghahfarokhi, A. Nezamzadeh-Ejhieh, Mater. Sci. Semicond. Process. 39 (2015) 265–275.
[32] A. Nezamzadeh-Ejhieh, A. Badri, Desalination 281 (2011) 248-256.
[33] A. Jodaei, A. Niaei, D. Salari, Korean J. Chem. Eng. 28 (2011) 1665–1671.
[34] F.J. Beltrán, F.J. Rivas, O. Gimeno, J. Chem. Technol. Biotechnol. 80 (2005) 973-984.
[35] C. Sahoo, A.K. Gupta, P. Anjali, Desalination 181 (2005) 91-100.
[36] B. Divband, M. Khatamian, G.R. Kazemi Eslamian, M. Darbandi, Appl. Sur. Sci. 284 (2013) 80-86.
[37] R. Georgekutty, M.K. Seery, S.C. Pillai, J. Phys. Chem. C 112 (2008) 13563-13570.

[38] M. Khatamian, Z. Alaji, Desalination 286 (2012) 248-253.
[39] Z. Ghasemi, H. Younesi, A.A. Zinatizadeh, J. Taiwan Inst. Chem. Eng. 65 (2016) 357–366.
[40] E. Evgenidou, K. Fytianos, I. Poulios, J. Photochem. Photobiol. A 175 (2005) 29–38.
[41] A. Nezamzadeh-Ejhieh, S. Khorsandi, J. Ind. Eng. Chem. 20 (2014) 937-946.
[42] K.M. Parida, S.S. Dash, D.P. Das, J. Colloid Interf. Sci. 298 (2006) 787.
[43] N. Ajoudanian, A. Nezamzadeh-Ejhieh, Mater. Sci. Semicond. Process. 36 (2015) 162-169.
[44] M. Babaahamdi-Milani, A. Nezamzadeh-Ejhieh, J. Hazard. Mater. 318 (2016) 291-301.
[45] J.H. Sun, Y.K. Wang, R.X. Sun, S.Y. Dong, Mater. Chem. Phys. 115 (2009) 303-308.
[46] M.J. Sadiq, A.S. Nesaraj, Iran. J. Catal. 4 (2014) 219-226.
[47] A. Nezamzadeh-Ejhieh, Z. Banan, Iran. J. Catal. 2 (2012) 79-83.